# Involvement of Metals in Enzymatic and Nonenzymatic Decomposition of C-Terminal α-Hydroxyglycine to Amide: An Implication for the Catalytic Role of Enzyme-Bound Zinc in the Peptidylamidoglycolate Lyase Reaction[†]

Kenichi Takahashi,[‡] Saori Harada,[‡] Yuichiro Higashimoto,[‡] Chizu Shimokawa,[‡] Hideaki Sato,[‡] Masakazu Sugishima,[‡] Yasuhiko Kaida,[§] and Masato Noguchi*,[‡]

*Department of Medical Biochemistry, Kurume University School of Medicine, Kurume 830-0011, Japan, and Biomass Technology Research Center, National Institute of Advanced Industrial Science and Technology, Tosu 841-0052, Japan*

ABSTRACT: The peptide C-terminal amide group essential for the full biological activity of many peptide hormones is produced by consecutive actions of peptidylglycine α-hydroxylating monooxygenase (PHM) and peptidylamidoglycolate lyase (PAL); PHM catalyzes the hydroxylation of C-terminal glycine, and PAL decomposes the peptidyl-α-hydroxyglycine to an amidated peptide and glyoxylate. PAL contains 1 mol of zinc, but its role, catalytic or structural, has not yet been clarified. In this study, we found that a series of transition metals, $Mn^{2+}$, $Co^{2+}$, $Ni^{2+}$, $Cu^{2+}$, $Zn^{2+}$, and $Cd^{2+}$, catalyze the nonenzymatic decomposition of the hydroxyglycine intermediate in a concentration-dependent manner. The second-order rate constant of the metal catalysis increased with elevation of pH, indicating that the hydrated metal acts as a general base. Extensive removal of the enzyme-bound metals remarkably diminished the PAL activity; $k_{cat}$ of the metal-depleted enzyme retaining 0.1 mol of zinc decreased to 3.2 $s^{-1}$ from 25.7 $s^{-1}$ of the wild-type enzyme. Among a series of divalent metals tested, $Zn^{2+}$, $Co^{2+}$, and $Cd^{2+}$ could fully restore the PAL activity of the metal-depleted enzyme. Especially, Zn substitution reproduced the steady-state parameters of the wild-type enzyme. On the other hand, Co and Cd substitution largely altered the kinetic parameters; the $k_{cat}$ increased 3- and 5-fold and the $K_m$ for the substrate increased 2.5- and 4-fold, respectively. These observations support that the enzyme-bound zinc plays a catalytic role, rather than a structural role, in the PAL reaction through the action of zinc-bound water as a general base.

The peptide C-terminal α-amide group, a unique structure occurring in many peptide hormones, is produced by an oxidative dealkylation of the C-terminal glycine residue existing in its precursor. This posttranslational modification is accomplished by two consecutive enzymes, peptidylglycine α-hydroxylating monooxygenase (PHM,[1] EC 1.14.17.3) and peptidylamidoglycolate lyase (PAL, EC 4.3.2.5) (*1*). First, the α-carbon of the C-terminal glycine is stereospecifically

Scheme 1: Peptidylglycine α-Amidating Reaction Catalyzed by Sequential Actions of PHM and PAL
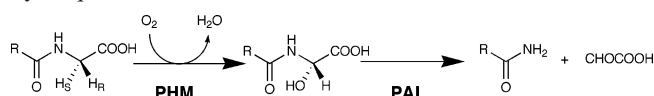


hydroxylated by PHM in an ascorbate- and copper-dependent manner (*2−5*). The resulting carbinol intermediate of *S*-configuration is then decomposed to the corresponding amidated peptide and glyoxylate by the second enzyme, PAL (Scheme 1) (*6, 7*). These two enzymes are originally encoded in a single mRNA and synthesized as a bifunctional enzyme in a single polypeptide. Therefore, the enzyme is sometimes designated bifunctional peptidylglycine α-amidating monooxygenase (bifunctional PAM), though in many cases PHM and PAL function as two distinct proteins as a result of limited proteolysis between the two catalytic domains (*8, 9*). The enzyme system, PHM and PAL, provides the only metabolic pathway responsible for the formation of the C-terminal amide of bioactive polypeptides. For about half of all peptide hormones, such as oxytocin and vasopressin, the C-terminal amide is indispensable for their full biological activity. It has been reported that deletion of these activities is lethal for *Drosophila* (*10*) and mouse (*11*).

Mechanically speaking, PHM is a typical monooxygenase; dioxygen is activated on the enzyme-bound copper by external electrons provided by ascorbate, and then the

* To whom correspondence should be addressed. Tel: 81-942-31-7544. Fax: 81-942-31-4377. E-mail: mnoguchi@med.kurume-u.ac.jp.

[‡] Kurume University School of Medicine.

[§] National Institute of Advanced Industrial Science and Technology.

[1] Abbreviations: εAca, ε-aminocaproic acid; EGTA, ethylene glycol bis(β-aminoethyl ether)-*N,N,N′,N′*-tetraacetic acid; HBTU, 1-[bis(dimethylamino)methylene]-1*H*-benzotriazolium 3-oxide hexafluorophosphate; HOBt, 6-chloro-1-hydroxybenzotriazole; ICP-AES, inductively coupled plasma atomic emission spectrometer; LpxC, UDP-3-*O*-((*R*)-3-hydroxymyristoyl)-*N*-acetylglucosamine deacetylase; PAL, peptidylamidoglycolate lyase; PAM, peptidylglycine α-amidating monooxygenase; PHM, peptidylglycine α-hydroxylating monooxygenase; TFA, trifluoroacetic acid; TNPYVG, *N*-2,4,6-trinitrophenyl-D-Tyr-L-Val-Gly; TNPYV-NH₂, *N*-2,4,6-trinitrophenyl-D-Tyr-L-Val-amide; TNPYV(OH)G, *N*-2,4,6-trinitrophenyl-D-Tyr-L-Val-(*S*)-α-hydroxy-Gly.

Scheme 2: Specific Acid and Base Catalysis for the C−N Cleavage of the Carbinol Intermediate
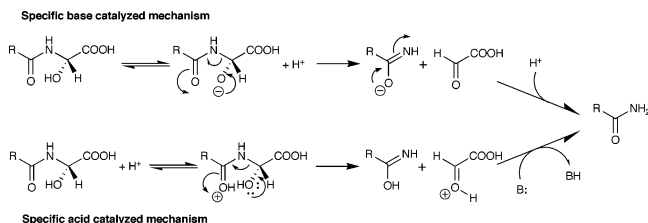


stereospecific substitution of the pro-S α-hydrogen of the C-terminal glycine with the hydroxyl group takes place, giving a carbinol intermediate. The PHM reaction has been extensively studied in relation to dopamine β-monooxygenase, a similar enzyme in the light of cofactor requirement, reaction mechanism, and sequence similarity (*1, 12*). In contrast to the well-characterized PHM, the PAL reaction has been poorly understood, and many mechanistic aspects have yet to be elucidated. The PAL reaction should proceed via acid- or base-catalyzed deprotonation of the hydroxyl moiety of the carbinol intermediate (Scheme 2) (*13*). Indeed, as early as 1991, Bundgaad and Kahns reported nonenzymatic base-catalyzed hydrolysis of peptidyl-α-hydroxyglycine derivatives (*14*), and more recently Mennenga et al. have reported the analyses of general buffer catalyzed C−N cleavage of carbinolamide and suggested the involvement of acid catalysis (*15*). In this context, the zinc, which is bound to the PAL domain at an approximately equimolar ratio, seems to be important for the catalysis, though the role of the metal has been controversial. A catalytic role has been proposed for zinc because of its coordination environment, such as two to three histidine ligands and one to two non-histidine O/N ligands (*16*). On the other hand, the structural zincs in proteins are generally thiolate-ligated (*16*). Kolhekar et al. suggested a structural role of the PAL-bound zinc based on the fact that treatment of PAL with divalent metal ion chelators increased its sensitivities to protease and heat (*17*).

The fact that chelating reagents, such as EDTA, remarkably decrease the PAL activity implies an essential role of metals in the reaction. However, there have been discrepancies between the inhibitory effects of chelating reagents and the degrees of restoration of PAL activity by exogenous metals (*16−19*). Bell et al. have reported that the decreased PAL activity in the presence of EDTA can be restored by adding an excess amount of Zn²⁺, Co²⁺, and Cd²⁺ (*16*). Other groups have reported that Ca²⁺, Mn²⁺, Fe²⁺, Ni²⁺, and Cu²⁺ are also able to restore the decreased PAL activity (*17−19*). From the ambiguities in the metal-restoring experiments reported in the literature, Kulathalia et al. have claimed that the inhibitory effect of EDTA on PAL is not due to metal chelation but due to direct binding of EDTA to PAL (*20*). Furthermore, Eipper's group (*21*) and we (*19*) have reported that a stoichiometric amount of calcium and a substoichiometric amount of iron are also bound to purified PAL protein, though their roles are still unknown. Thus, clarification of the role of these metals in the PAL activity is a major issue for understanding its reaction mechanism.

In this study, we first describe that a series of divalent metals such as Mn²⁺, Co²⁺, Ni²⁺, Cu²⁺, Zn²⁺, and Cd²⁺ themselves are capable of catalyzing the nonenzymatic decomposition of the carbinol intermediate to amidated peptide at neutral pH. Their action is shown to be a general

base catalysis by hydrated metals. Then, to explore how the enzyme-bound metals are involved in the PAL reaction, we prepared a metal-depleted PAM and attempted to reconstitute the enzyme with exogenous metal. The remarkably diminished PAL activity by extensive metal removal is fully restored only by substitution with Zn²⁺, Co²⁺, and Cd²⁺. On the basis of these findings, we will discuss the role of the enzyme-bound zinc in the PAL reaction.

## MATERIALS AND METHODS

*Chemicals and General Methods.* Chemicals were purchased from commercial sources as specified (*19, 22, 23*) unless otherwise noted and used without further purification. All glassware was washed with nitric acid prior to use. All buffers and distilled water used for metal substitution experiments were passed through a 10 cm column of Chelex resin (Bio-Rad). Na₂SO₄, CaCl₂·2H₂O, MnSO₄·5H₂O, FeCl₂·4H₂O, CoSO₄·7H₂O, NiSO₄·6H₂O, CuSO₄·2H₂O, ZnSO₄·7H₂O, and CdCl₂·2.5H₂O were purchased from Nacalai Tesque (Kyoto, Japan). Trace metal analysis was performed with an inductively coupled plasma atomic emission spectrometer (ICP-AES) (SPS 1200 AR plasma spectrometer; SEIKO Instruments, Tokyo, Japan) employing the standard metal solutions commercially available. Metal contents in protein were corrected for contaminations in buffer, though they were usually negligible. Sulfolink coupling gel was purchased from Pierce; Fmoc-Gly-wang-resin LL was from Calbiochem. *N*-2,4,6-Trinitrophenyl-D-Tyr-L-Val-Gly (TNPYVG) and *N*-2,4,6-trinitrophenyl-D-Tyr-L-Val-(*S*)-α-hydroxy-Gly (TNPYV(OH)G) were synthesized from D-Tyr-L-Val-Gly (Sigma) as described previously (*19*). Argon gas (>99.9999%) was passed through a basic solution of pyrogallol to scrub oxygen. Buffers and protein solutions used in anaerobic experiments were degassed either by bubbling with oxygen-scrubbed argon or by stirring or gentle agitation under a stream of oxygen-scrubbed argon for at least 6 h. Data are presented as an average ± the standard error based on at least three independent assays unless otherwise stated.

*Metal-Catalyzed Nonenzymatic Decomposition of TNPYV (OH)G to TNPYV-NH₂.* Typically, a 150 $\mu$L reaction mixture containing 16 $\mu$M TNPYV(OH)G, 1% methanol, 100 mM MES/NaOH, pH 5.5, 6.0, 6.5, or 7.0, and 0−100 mM divalent metal cation was incubated at 25 °C for 6−48 h; ionic strength (*I*) was adjusted to 1.0 with KCl. At desired time points, a 50 $\mu$L aliquot of the reaction mixture was mixed with a 150 $\mu$L stop solution, 0.67% (v/v) TFA and 53.3% (v/v) acetonitrile, and then the percent conversion of TNPVV(OH)G to TNPYV-NH₂ was determined by HPLC as described (*19*). The observed first-order rate constant of metal-catalyzed reaction, $k_{obs}$, was calculated by fitting the time course of the conversion reaction to the equation:

$$k_{obs}t = -\ln(1 - P/A_0) \qquad (1)$$

where $A_0$ and $P$ stand for the initial substrate concentration (16 $\mu$M) and the concentration of the product at time $t$, respectively. When the percent conversion of substrate to product was less than 5%, $k_{obs}$ was calculated by the equation:

$$k_{obs}t = P/A_0 \qquad (2)$$

*Preparation of Substrate Affinity Resin.* The synthesis of a substrate analogue, Cys-εAca-εAca-Phe-Phe-Gly, was

carried out by the standard solid-phase method with Fmoc-Gly-wang-resin as a starting material. After removal of the Fmoc group from the starting material, Fmoc-L-Phe, Fmoc-L-Phe, *N*-Fmoc-εAca, *N*-Fmoc-εAca, and Fmoc-L-Cys were sequentially coupled by HOBt and HBTU and deprotected by 20% (v/v) piperazine to obtain Cys-εAca-εAca-Phe-Phe-Gly. Cleavage of the peptide from the resin was accomplished by TFA. Purification of the peptide was performed on a Waters 600E multisolvent system equipped with a 600 controller and a 996 photodiode array detector. A Cosmosil C18 column (4.6 × 250 mm; Nacalai Tesque) was used with a solvent system consisting of 0.1% TFA (solvent A) and 80% (v/v) acetonitrile in 0.1% TFA (solvent B). With a linear gradient from 0% to 60% of solvent B over 45 min at a flow rate of 1 mL/min, Cys-εAca-εAca-Phe-Phe-Gly was eluted as a single peak at a retention time of 23 min. The substrate affinity resin was prepared by mixing 1 mg of the synthesized peptide to 1 mL of Sulfolink coupling gel; the sulfhydryl group of the peptide was coupled to the iodoacetyl group at the end of a spacer arm fixed to the Sulfolink coupling gel. The remaining iodoacetyl group was blocked by L-Cys.

*Enzyme Expression and Purification.* A soluble form of human bifunctional PAM consisting of 834 amino acids, which lacks the C-terminal 139 amino acid stretch including the membrane binding domain, was stably expressed in CHO cells as described by Satani et al. (*19*). In the present study, however, EX-CELL 302 (JRH Biosciences, Lenexa, KS), instead of EX-CELL 301, was used as the serum-free culture medium. The purification of the protein was carried out as described (*19*) with modifications.

The active fraction (usually ca. 150 mL) eluted from the phenyl-Sepharose column (*19*) was applied on a substrate affinity column (2.5 × 3 cm) equilibrated with 20 mM MES/KOH, pH 6.0, containing 0.5 M NaCl at a flow rate of 2.5 mL/min. After being washed with 75 mL of the equilibrating buffer, protein was eluted by 16 mM MES/KOH, pH 6.0, and 0.4 M NaCl containing 20% (v/v) acetonitrile. After acetonitrile in the active fraction (usually ca. 30 mL) was evaporated under a nitrogen stream, the protein solution was concentrated with the aid of Centriprep YM-10 (10 kDa MWCO; Millipore) and then fractionated on a Sephacryl S-300 column (1.5 × 115 cm) equilibrated with 20 mM HEPES/NaOH, pH 7.2, containing 0.1 M NaCl and 0.01% Tween 20. This three-step purification usually yielded 1−2 mg of purified PAM protein (>95% purity as judged on silver-stained SDS−PAGE) from 1 L of spent medium of the conventional roller bottle culture (*19*). Protein concentrations were determined by BCA assay (Pierce) using BSA as a standard.

*Removal of PAM-Bound Metals.* This was performed principally according to the method previously described (*24−26*) with modifications. All procedures were carried out at 4 °C, and all buffers and reagents were degassed prior to use. Addition of reagents and exchange of buffers were carried out in a glovebox filled with nitrogen. Typically, 2 mL of 1 mg/mL PAM was introduced into a Slide-A-Lyzer cassette (10 kDa cutoff; Pierce) with a syringe, and the cassette was immersed in a separable flask containing 400 mL of dialyzing buffer, 25 mM MES/NaOH, pH 6.0, and 1 mM each of EDTA and EGTA; the separable flask was covered by a roof that bore three ground glass joints and

then placed on a SWC-900 cool stirrer (Nissin Rika, Tokyo, Japan) (see Supporting Information, Figure S1). During dialysis, the dialyzing buffer was kept anaerobic by continuous bubbling of oxygen-scrubbed argon through a gas dispersion tube with fritted cylinder that was tightly attached to one of the ground glass joints. One of the other two ground glass joints was used for releasing argon through a two-way cock, and the remaining joint was usually plugged with a temperature probe; additions of reagents were made through this port. At 2 h after the dialysis was started, KCN (1 mM) and ascorbate (55 μM, 1000 equiv to PAM) were added to the dialyzing buffer, and the dialysis was continued for 6−16 h. This dialyzing manipulation was repeated three times. The protein solution was finally dialyzed for 36 h, with two changes of the buffer, against 400 mL of 25 mM MES/NaOH, pH 6.0, containing 1.3 g of Chelex resin (0.4 mmol as iminodiacetate); the last 12 h dialysis was carried out in the air. The protein was then removed from the Slide-A-Lyzer cassette with a syringe to give a metal-depleted PAM.

*Assay of the PAL Reaction.* The measurement of PAL activity was performed as described (*19*). For steady-state analyses, the concentration of TNPYV(OH)G was varied from 9 to 480 μM. A 200 μL reaction system contained 100 mM MES/NaOH, 1% methanol, and TNPYV(OH)G. After the preincubation at 37 °C for 5 min, the reaction was started by adding the enzyme (40 ng/mL) at 37 °C. At desired time points, a 50 μL aliquot of the reaction mixture was mixed with a 150 μL stop solution, 0.67% (v/v) TFA, and 53.3% (v/v) acetonitrile and then analyzed by HPLC as described (*18*). Reaction times were varied depending on the substrate concentration and the level of PAL activity, so that the percent conversion of TNPYV(OH)G would not exceed 10%; reaction times were 1−14 min for the wild-type, Zn-, Co-, and Cd-substituted PAM and 14−28 min for Ni-substituted and the metal-depleted PAM. The initial velocities thus obtained for respective PAM preparations were fitted to the Michaelis−Menten equation by nonlinear regression using Kaleidagraph 4.0 (Synergy Software).

## RESULTS

*Metal-Catalyzed Decomposition of TNPYV(OH)G to TNPYV-NH₂.* In the course of the investigation of nonenzymatic decomposition of TNPYV(OH)G to TNPYV-NH₂, we found that this reaction was greatly accelerated by addition of such divalent metals as $Mn^{2+}$, $Co^{2+}$, $Ni^{2+}$, $Cu^{2+}$, $Zn^{2+}$, and $Cd^{2+}$. In the presence of these metals, the reaction rate was enhanced ca. 20-fold at the maximum, though it varied depending on the metal species added; $Ca^{2+}$ showed a similar effect but was much less effective compared to the metals listed above (data not shown). As shown in Figure 1, observed first-order rate constants ($k_{obs}$) of the metal catalysis increased in a concentration-dependent manner. In addition, the slope of each $k_{obs}$ curve became steeper at higher pH, indicating that the apparent second-order rate constant of the metal catalysis increased depending on the elevation of pH. Basically, the carbinol intermediate more rapidly decomposes to the corresponding amidated peptide at higher pH (*7, 18, 22*), though it is quite stable at neutral to acidic pH (*27*). In fact, $k_{obs}$ of the metal-independent decay of TNPYV(OH)G to TNPYV-NH₂ gradually increased along with the elevation of pH (see the intersections across the vertical axes of Figure
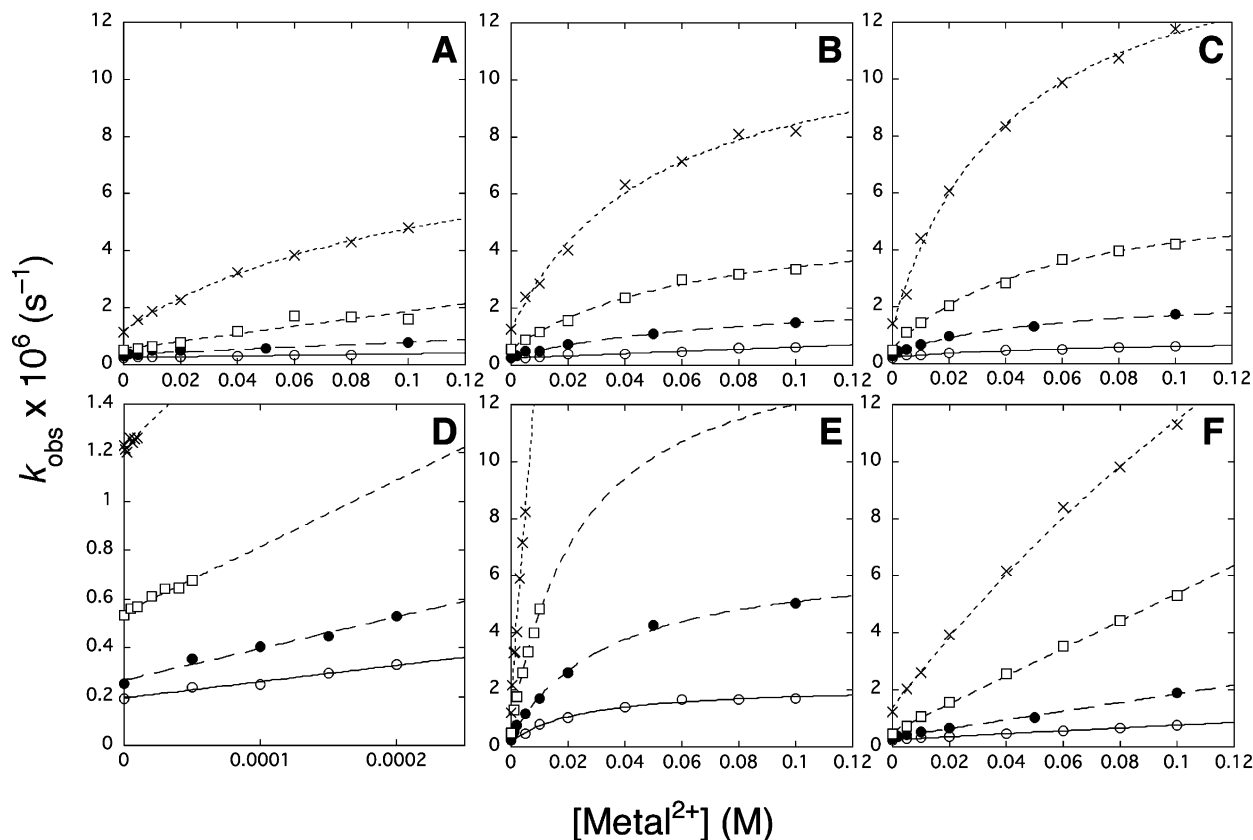
FIGURE 1: Metal-catalyzed decomposition of TNPYV(OH)G to TNPYV-NH$_2$ at various pHs. The reactions were carried out at 25 °C for 6−36 h under the following conditions: 100 mM MES/NaOH, pH 5.5 (○), 6.0 (●), 6.5 (□), or 7.0 (×), 1% methanol, 16 $\mu$M TNPYV(OH)G, $I$ = 1.0 (KCl), and varied concentrations of (A) MnSO$_4$, (B) CoSO$_4$, (C) NiSO$_4$, (D) CuSO$_4$, (E) ZnSO$_4$, or (F) CdCl$_2$. The reaction by copper (D) was carried out in the presence of a much lower concentration of the metal than that of others, because the solubility of cupric ion was quite low especially at higher pH. The observed first-order rate constant ($k_{obs}$) was plotted as a function of the metal concentration.

1); those values were $2.4 \times 10^{-7}$, $3.3 \times 10^{-7}$, $5.5 \times 10^{-7}$, and $1.3 \times 10^{-6}$ s$^{-1}$ at pH 5.5, 6.0, 6.5, and 7.0, respectively. Nevertheless, the apparent second-order rate constant of the metal-catalyzed reaction obviously increased by elevating pH. These observations indicate that the reaction is stimulated by general base catalysis of metal-bound water.

Most of the plots of $k_{obs}$ versus the metal concentrations showed hyperbolic curves (Figure 1). This behavior may allude to a kind of association-dissociation equilibrium between the TNPYV(OH)G and the hydrated metal preceding the catalysis (see Discussion for details). Under the present condition, whereby the metal concentration ([M$^{2+}$]) was varied at millimolar order and far exceeded the fixed concentration of TNPYV(OH)G (16 $\mu$M), the $k_{obs}$ can be approximated by the equation:

$$k_{obs} = k_2{}^{app}[\text{M}^{2+}]/(1 + [\text{M}^{2+}]/K_D) + k_{bkg} \qquad (3)$$

where $k_{bkg}$ is the observed first-order rate constant in the absence of metal, $K_D$, a dissociation constant between metal and the carbinol intermediate, and $k_2{}^{app}$, the apparent second-order rate constant for the metal catalysis. Thus the value of $k_2{}^{app}$ was obtained by nonlinear regression of the plot to eq 3. In the cases where $k_{obs}$ linearly correlates to [M$^{2+}$], such as the reactions with Mn$^{2+}$ and Cd$^{2+}$ at lower pH (Figure 1A,F), $k_2{}^{app}$ was simply calculated as the slope of the linear regression of the plot. The values of $k_2{}^{app}$ thus obtained are summarized in Table 1.

Once $k_2{}^{app}$ was determined, the second-order rate constant of the catalysis by the basic form of the hydrated

Table 1: Apparent Second-Order Rate Constants ($k_2{}^{app}$) for Metal-Catalyzed Decomposition of TNPYV(OH)G to TNPYV-NH$_2$[a]

| metal | $k_2{}^{app}$ ($\pm$SE) $\times$ 10$^6$ (M$^{-1}$ s$^{-1}$) | | | |
|---|---|---|---|---|
| | pH 5.5 | pH 6.0 | pH 6.5 | pH 7.0 |
| Mn$^{2+}$ | 1.27 ± 0.08 | 4.29 ± 0.57 | 13.1 ± 2.0 | 66.9 ± 4.9 |
| Co$^{2+}$ | 3.77 ± 1.13 | 23.7 ± 3.6 | 73.2 ± 9.2 | 213 ± 31 |
| Ni$^{2+}$ | 8.77 ± 2.12 | 39.2 ± 4.5 | 106 ± 11 | 346 ± 35 |
| Cu$^{2+}$ | 669 ± 56 | 1300 ± 100 | 2710 ± 230 | 6380 ± 900 |
| Zn$^{2+}$ | 77.1 ± 12.1 | 186 ± 12 | 577 ± 75 | 1600 ± 270 |
| Cd$^{2+}$ | 5.02 ± 0.16 | 15.2 ± 0.5 | 48.3 ± 0.8 | 131 ± 10 |

[a] In 100 mM MES/NaOH, 1% methanol, $I$ = 1.0 (KCl), 25 °C. The $k_2{}^{app}$ values were calculated as described in the Results section.

metal, $k_2$, was obtained by plotting the $k_2{}^{app}$ values against the fraction of the basic form of corresponding hydrated metals, which was calculated based on p$K_a$ values of hydrated metals available in the literature (28); the slope of the least-squares linear regression of the plot gave the $k_2$ values (Supporting Information, Table S1 and Figure S2). Figure 2 represents the Brønsted correlation between the acidity of the hydrated metal and log $k_2$, from which a $\beta$ value of 0.30 ± 0.06 was obtained. This value indicates a moderately substrate-like transition state structure, rather than a symmetric one, in the course of proton transfer from the α-hydroxy group of the carbinol intermediate to the catalytic base, metal-bound hydroxide. A point for the hydroxide ion-catalyzed reaction (the second-order rate constant for the hydroxide ion-catalyzed reaction, $k_{2,OH}$, was determined to be 5.3 ± 0.9 M$^{-1}$ s$^{-1}$;
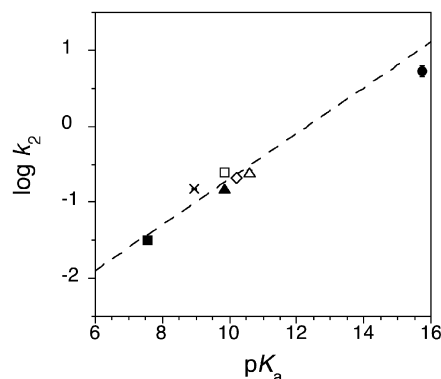
FIGURE 2: The Brønsted plot of metal-catalyzed decomposition of TNPYV(OH)G to TNPYV-NH$_2$. The logarithms of the second-order rate constants ($k_2$) for the catalysis by the basic form of hydrated metals were plotted as a function of p$K_a$ of the metal. The $k_2$ values were obtained as described in the text (see Supporting Information, Figure S2 and Table S1). The p$K_a$ values of each metal were assumed to be 10.59 (Mn$^{2+}$, △), 9.85 (Co$^{2+}$, ▲), 9.86 (Ni$^{2+}$, □), 7.54 (Cu$^{2+}$, ■), 8.96 (Zn$^{2+}$, ×), and 10.2 (Cd$^{2+}$, ◇) under the reaction conditions (25 °C, $I = 1.0$) (*29*). The metal-independent hydroxide ion-catalyzed reaction ($k_{2,OH}$, ●) is also plotted (see Supporting Information, Figures S3 and S4 and Table S2). The line is a linear regression of the plots only for metal catalysis, not including the plot for the hydroxide ion catalysis.

see Supporting Information, Figures S3 and S4 and Table S2) is also included in Figure 2 and shows a good correlation with the points for the metal-catalyzed reaction.

*Analysis of PAM-Bound Metals and Removal of Them from PAM.* ICP-AES analysis of three independent PAM preparations showed that each of them invariably contained approximately 0.83 mol of zinc, 0.46 mol of copper, 1.15 mol of calcium, and 0.42 mol of magnesium per mole of PAM (Table 2); the copper must originate from the PHM domain of PAM. A nonnegligible amount of iron was also detected as previously reported (*19, 21*), though its content varied from 0.31 to 0.67 mol/mol of PAM between the preparations. The PAL activity of the each preparation, however, was not proportional to the iron contents (data not shown). To investigate the roles of these metals in the PAL reaction, we attempted to prepare extensively metal-depleted enzymes and to restore them with exogenous metals. The dialysis against the buffer containing EDTA, EGTA, and KCN under the reducing condition removed most of the Ca$^{2+}$, Cu$^{2+}$, and Zn$^{2+}$ and a majority of the Mg$^{2+}$ from the enzyme (Table 2). In contrast, the iron was still retained at nearly the original level, suggesting that the iron is deeply embedded inside the protein so that the chelating reagents may have difficulty accessing the binding site. As presented in Table 3, activity of the metal-depleted PAM was only 10% that of the original PAL activity; $k_{cat}$ decreased from 25.7 to 3.2 s$^{-1}$, $K_m$ increased from 21.5 to 90 $\mu$M, and, as a result, $k_{cat}/K_m$ decreased 30-fold. These findings indicate that the metal(s) was (were) absolutely indispensable to the PAL reaction.

*Restoration of PAL Activity by Divalent Metals.* The bifunctional PAM is supposed to possess at least three metal binding sites: one in the PAL domain for zinc and the other two in the PHM domain for copper. At first, we tried to reconstitute the metal-depleted PAM by incubating the protein with 5 mol equiv of metals in the presence of 25 mM MES/NaOH, pH 6.0, at 25 °C for 2 h, but this trial failed to restore the PAL activity. Therefore, we

attempted to incubate the metal-depleted PAM with much higher concentrations of metals (Figure 3). Fe$^{2+}$ was not examined in this study because the ferrous state could not be completely maintained during the restoration. As expected, Zn$^{2+}$ restored the PAL activity at 200−500 $\mu$M, showing 130% of the activity of the wild-type enzyme. At pH 6.0, the contribution of free Zn$^{2+}$ to product formation should be negligible, because millimolar order of Zn (>10 mM) is needed to clearly detect the nonenzymatic Zn$^{2+}$-catalyzed reaction (compare Table 1 and Figure 3). Co$^{2+}$ and Cd$^{2+}$, which were not detected in the wild-type enzyme, were also able to fully restore the PAL activity; these metals showed 220% and 180% restoration of the original activity, respectively. The concentration of Cd$^{2+}$ required for the full restoration was higher than that of Co$^{2+}$ and Zn$^{2+}$, presumably reflecting the difference of affinity of these metals to the protein. Ni$^{2+}$ showed only 30% restoration, and Ca$^{2+}$, Mg$^{2+}$, Mn$^{2+}$, and Cu$^{2+}$ had no effect (Figure 3).

*Steady-State Analysis of PAL Activity of Metal-Substituted PAM.* Since the Co-, Zn-, and Cd-substituted PAMs showed a full restoration of PAL activity, we made a further characterization of these metal-substituted enzymes. Figure 4 shows the steady-state kinetics of their PAL activity, and Table 3 summarizes the kinetic parameters. Substitution of metal-depleted PAM by Zn$^{2+}$ almost reproduced the PAL activity of the wild-type enzyme with respect to all of the steady-state parameters. On the other hand, Co and Cd substitutions increased the $k_{cat}$ approximately 3- and 5-fold and also increased the $K_m$ 2.5- and 4-fold compared to the wild-type enzyme, respectively. Ni substitution brought about only 30% recovery of $k_{cat}$, while $K_m$ did not change from that of the metal-depleted enzyme. The $k_{cat}/K_m$ values showed little difference between the wild-type, Zn-, Co-, and Cd-substituted PAM.

When the wild-type PAM was incubated with 0.5 mM CoSO$_4$ or 1 mM CdCl$_2$, the $k_{cat}$ and $K_m$ of the metal-treated wild-type PAM slightly increased; $k_{cat} = 32.8 \pm 1.5$ s$^{-1}$ and $K_m = 42.4 \pm 7.2$ $\mu$M for Co$^{2+}$-treated PAM, $k_{cat}$ of 34.1 $\pm$ 2.6 s$^{-1}$ and $K_m$ of 42.2 $\pm$ 11.5 $\mu$M for Cd$^{2+}$-treated PAM. These increases of the kinetic parameters are probably due to binding of Co$^{2+}$ or Cd$^{2+}$ to empty zinc-binding sites on PAL (note that the purified wild-type PAM invariably contained ca. 0.8 mol of zinc/mol of PAM (Table 2). In fact, when the wild-type PAM was incubated with exogenous zinc, $k_{cat}$ slightly increased from 25.7 $\pm$ 0.4 to 29.7 $\pm$ 2.2 s$^{-1}$ without significant change of $K_m$ (from 21.5 $\pm$ 1.3 to 20.8 $\pm$ 4.8 mM). These findings indicate that the zinc ions bound to the active site on the wild-type PAL cannot be easily replaced by exogenous Co$^{2+}$ or Cd$^{2+}$ and that these metals can restore the PAL activity of the metal-depleted PAM by occupying the same binding sites for zinc.

## DISCUSSION

*Metal-Catalyzed Decomposition of TNPYV(OH)G to TNPYV-NH$_2$.* The present study revealed that the hydrated metal itself can catalyze the nonenzymatic conversion of TNPYV(OH)G to TNPYV-NH$_2$. For this reaction two catalytic mechanisms will be considered: (1) metal-bound hydroxide serves as a catalytic base and (2) the metal acts as an electrophilic catalyst (Scheme 2). The latter pos-

Table 2: Molar Ratios of Divalent Metals Bound to PAM[a]

| | Mg | Ca | Mn | Fe | Co | Ni | Cu | Zn | Cd |
|---|---|---|---|---|---|---|---|---|---|
| | | | | $[M^{2+}]/[E]$ | | | | | |
| wild type | $0.42 \pm 0.05$ | $1.15 \pm 0.05$ | $0.01 \pm 0.00$ | $0.49 \pm 0.18$ | $<0.02$ | $<0.04$ | $0.46 \pm 0.05$ | $0.83 \pm 0.04$ | $<0.01$ |
| metal depleted | $0.18 \pm 0.05$ | $0.00 \pm 0.00$ | $0.01 \pm 0.00$ | $0.46 \pm 0.17$ | $<0.02$ | $<0.04$ | $<0.01$ | $0.11 \pm 0.01$ | $<0.01$ |

[a] For the measurement of the content of each metal, 45.5 $\mu$g of wild-type or metal-depleted PAM was used.

Table 3: Summary of Steady-State Kinetic Parameters for PAL Activities of Wild-Type, Metal-Depleted, and Metal-Substituted PAMs

| prep | $k_{cat}$ (s$^{-1}$) | $K_m$ ($\mu$M) | $k_{cat}/K_m \times 10^{-6}$ (M$^{-1}$ s$^{-1}$) |
|---|---|---|---|
| wild type | $25.7 \pm 0.4$ | $21.5 \pm 1.3$ | $1.2 \pm 0.1$ |
| metal depleted | $3.2 \pm 0.6$ | $88.7 \pm 45.4$ | $0.036 \pm 0.013$ |
| $Zn^{2+}$ | $29.8 \pm 0.6$ | $13.4 \pm 1.3$ | $2.2 \pm 0.2$ |
| $Co^{2+}$ | $87.3 \pm 1.2$ | $50.3 \pm 2.4$ | $1.7 \pm 0.1$ |
| $Ni^{2+}$ | $9.1 \pm 0.9$ | $98.0 \pm 26.3$ | $0.093 \pm 0.017$ |
| $Cd^{2+}$ | $127 \pm 7$ | $74.6 \pm 12.7$ | $1.7 \pm 0.2$ |

sibility was raised by a recent study in which *N*-(hydroxymethyl)benzamide derivatives, an analogue of the carbinol intermediate, were shown to be decomposed by buffer-mediated general acid catalysis (*13, 15*). However, the fact that the second-order rate constant of metal catalysis was increased by elevating pH clearly indicates that the reaction is stimulated by general base catalysis of metal-bound water probably through deprotonation of the hydroxyl group of the carbinol intermediate (Figure 1).

Most of the plots of the observed first-order rate constant ($k_{obs}$) versus the metal concentration ([$M^{2+}$]) were hyperbolic curves (Figure 1). This can be explained by a rapid association and dissociation equilibrium between the substrate and the hydrated metal prior to the rate-determining catalytic step. This presumption is consistent with the fact that the plots of $k_{obs}$ versus [$M^{2+}$] were well
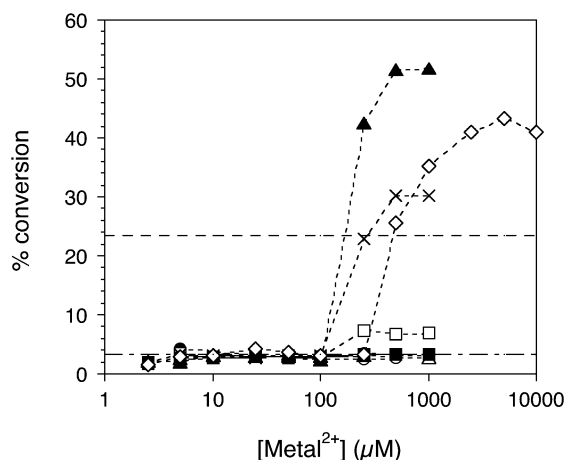


FIGURE 4: Steady-state kinetics of the PAL activity of metal-substituted PAMs. The metal-substituted PAMs were obtained by incubating 0.83 $\mu$M metal-depleted PAM with 0.5 mM ZnSO$_4$, 0.5 mM CoSO$_4$, 1 mM CdCl$_2$, or 0.5 mM NiSO$_4$ in 25 mM MES/NaOH, pH 6.0, at 25 °C for 2 h. The protein solution was diluted to 100 ng/mL with 100 mM MES/NaOH, pH 6.0, which had been warmed to 37 °C, and then immediately subjected to the PAL assay. Reactions were carried out at 37 °C in the presence of 100 mM MES/NaOH, pH 6.0, 1% methanol, indicated concentrations of TNPYV(OH)G, 0.44 nM each wild-type PAM (●), metal-depleted PAM (○), Zn-PAM (×), Co-PAM (▲), Cd-PAM (◇), and Ni-PAM (□). The initial velocity that had been normalized to PAL concentration was plotted as a function of TNPYV(OH)G concentration. The lines were a theoretical fitting to the Michaelis−Menten equation.

fitted to eq 3. Actually, a similar mechanism has been proposed for solvent−ligand interchange reaction between hydrated metal, $M(OH_2)_x^{n+}$, and exogenous ligand, L (*29*):

$$M(OH_2)_x^{n+} + L \underset{K_D}{\rightleftharpoons} M(OH_2)_x^{n+}], L \xrightarrow{k_i}$$

$$M(OH_2)_{x-1}L^{n+} + H_2O$$
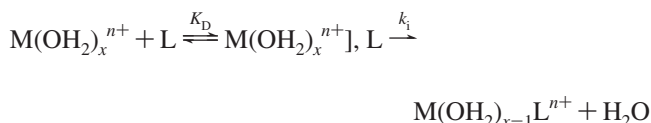
where $k_i$ is the reaction rate constant for ligand interchange and $K_D$ is the dissociation constant between $M(OH_2)_x^{n+}$ and L. In this mechanism, the reaction rate is rationally expressed by the equation (*29*):

$$d[M(OH_2)_{x-1}{}^{n+}L]/dt = (k_i/K_D)[M(OH_2)_x^{n+}][L]/(1 + [L]/K_D) \tag{4}$$

Equation 3 has been simply derived from eq 4. Since the metal-catalyzed decomposition of TNPYV(OH)G to TNPYV-NH$_2$ would start with the interaction of water molecules bound to the primary solvation shell with the substrate hydroxyl group as is the case with the ligand interchange reaction, it is fully conceivable that both reactions shared the same mechanism. The apparently linear correlation between $k_{obs}$ and [$M^{2+}$] observed in some cases would reflect the fact that the $K_D$ was much larger than the substrate concentration employed (Figure 1D,F).



FIGURE 3: Restoration of PAL activity by divalent metal ions. The metal-depleted PAM (0.83 $\mu$M, 75.7 $\mu$g of protein/mL) was incubated in 25 mM MES/NaOH, pH 6.0, and the indicated concentrations of MgSO$_4$ (○), CaCl$_2$ (●), MnSO$_4$ (△), CoSO$_4$ (▲), NiSO$_4$ (□), CuSO$_4$ (■), ZnSO$_4$ (×), or CdCl$_2$ (◇) at 25 °C for 2 h. The protein solution was diluted to 100 ng/mL with 100 mM MES/NaOH, pH 6.0, which had been warmed to 37 °C, and then immediately subjected to the PAL assay. The reactions were carried out at 37 °C for 30 min in 100 mM MES/NaOH (pH 6.0), 1% methanol, 16 $\mu$M TNPYV(OH)G, and 40 ng/mL (0.44 nM) PAM. The percent conversion from TNPYV(OH)G to TNPYV-NH$_2$ was plotted against metal concentrations. The horizontal lines indicate the percent conversion by wild-type (---) and metal-depleted (− -−) PAMs under the same condition.
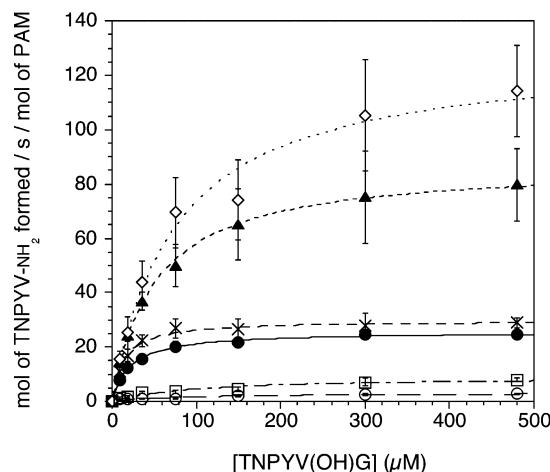
The Brønsted $\beta$ value of 0.30 (Figure 2) suggests that the moderately substrate-like transition state lies in the process of proton transfer from substrate to metal-bound hydroxide. It should be noteworthy that the second-order rate constant of the hydroxide ion-catalyzed reaction, $k_{2,OH} = 5.3$ M$^{-1}$ s$^{-1}$, is in a good correlation with that of the metal-catalyzed reaction (Figure 2). This observation indicates that the metal-catalyzed reaction should proceed via the same mechanism as the hydroxide-catalyzed reaction.

*Removal and Substitution of Enzyme-Bound Metals.* The dialysis against EDTA, EGTA, and KCN in the presence of ascorbate under anaerobic conditions yielded extensively metal-depleted PAM, though the enzyme still retained the original level of iron and 0.1 mol of zinc per mole of PAM (Table 2). Removal of enzyme-bound zinc is often difficult because zinc is firmly bound to enzymes in general (30, 31). One of the most successful cases for zinc removal has been reported in the study of UDP-3-*O*-((*R*)-3-hydroxymyristoyl)-*N*-acetylglucosamine deacetylase (LpxC), a zinc-containing enzyme responsible for the biosynthesis of lipid A, a bacterial endotoxin. However, the zinc-depleted LpxC still retained a comparable level of residual zinc as our metal-depleted PAM, 0.05−0.1 mol/mol of LpxC (32).

The PAL activity was dramatically diminished by removal of metals from the wild-type PAM; $k_{cat}$ decreased from 25.7 to 3.2 s$^{-1}$ (Table 3). The remaining activity was probably due to the residual zinc. In the previous studies of the metal requirements for the PAL activity, chelating agents such as EDTA were directly added to the PAL assay mixture to observe the loss of PAL activity, and then excess amounts of various metals were subsequently added to examine the recovery of the PAL activity (16−19). However, as Vallee and Auld pointed out, the inhibition of an enzyme by a chelating agent does not constitute conclusive evidence that it is a metalloenzyme, nor does the failure to observe inhibition with chelating agents necessarily reflect the absence of either zinc or another metal. Only metal analysis can definitively prove either (30). In this study, we were able to demonstrate the absolute requirement of the metal in the PAL reaction by clarifying the relation between the residual PAL activity of metal-depleted PAM and the level of remaining metal.

The addition of zinc to the metal-depleted PAM fully restored the PAL activity and reproduced the steady-state parameters of the wild-type enzyme (Figures 3 and 4 and Table 3). The $k_{cat}$ value and the activity of Zn-reconstituted PAM were 20−30% higher than those of the wild-type PAM. Similar elevation of $k_{cat}$ was also seen in the wild-type PAM supplemented with zinc. This result should be plausible because the PAL activity was roughly proportional to the zinc content; the metal-depleted PAM containing 0.1 mol of zinc showed one-eighth of the PAL activity of the wild-type enzyme containing 0.8 mol of zinc. The 20−30% elevation of the $k_{cat}$ by exogenous zinc implies that the metal-depleted PAM would be reconstituted with an equimolar amount of zinc.

Cobalt and cadmium were also able to fully restore the PAL activity of the metal-depleted PAM, while other metals, Ni$^{2+}$, Mn$^{2+}$, Cu$^{2+}$, Ca$^{2+}$, and Mg$^{2+}$, were of practically no use (Figure 2). However, previous studies (17−19) reported that the above divalent metals had shown a substantial restoring activity for EDTA-treated enzyme. The discrepancy

between the previous and the present studies may reside in the difference in the experimental procedures as stated above. Chelating reagents could inhibit the PAL activity by peeling off the enzyme-bound zinc as well as by direct binding to the PAL protein. The direct addition of metals to EDTA-containing enzyme solution may restore the PAL activity merely by facilitating dissociation of EDTA from the enzyme protein. Thus, the restoring activity of the various metals seen in the previous studies may not necessarily imply their direct binding to the PAL active site. In this study, for the first time, strict metal selectivity for PAL activity has been shown with the metal-depleted enzyme.

For the full restoration of PAL activity with zinc, a high concentration of the metal ($>200$ $\mu$M) was required. Usually, one equimolar dose of zinc is enough to fully restore mononuclear zinc hydrolases, such as carboxypeptidase A (37, 38) D-aminoacylase (39), and LpxC (32). Rather, excess zinc is inhibitory (32, 33, 37−39); the inhibitory effect is ascribed to binding of the metal to a second zinc binding site in the vicinity of the catalytic one (33). The following common zinc binding motifs have been found in the zinc enzyme superfamilies: **HEXXH** in the zinc $\alpha,\beta$-hydrolase superfamily (e.g., carboxipeptidase A (33)), **HXH** in the zinc $\alpha/\beta$-barrel amidohydrolase superfamily (e.g., D-aminoacylase (39)), and **HKX(L,F)D** in LpxCs (40) (the amino acids in bold face are direct zinc ligands). Interestingly, PAL lacks any of these common zinc binding motifs. This may partially account for the requirement of a high concentration of zinc for full restoration of the PAL activity.

*Role of Zinc in the PAL Reaction.* Is the role of zinc bound to PAL structural or catalytic? In either case, removal of zinc would lead to loss of the activity. Since no structural information of the PAL domain is available at present, both possibilities should be considered. Basically, the structural zinc is accommodated in a compact domain, whereby the zinc is liganded typically by four cysteine residues in a tetrahedral geometry (34, 35). On the other hand, catalytic zinc ion is generally coordinated with four ligands, i.e., three atoms of N, O, or S (His, Cys, Asp, or Glu) and a water molecule as a fourth ligand, though five- or six-coordinated forms are also known (31, 33). These ligands enhance the electrophilicity of zinc and lower the p$K_a$ of Zn$^{2+}$-bound water to facilitate nucleophilic attack on the substrate carbonyl carbon, as is well documented in the reactions of zinc hydrolases (33) and carbonic anhydrase (36). The coordination state of the zinc bound to PAL consisting of only O/N ligand with two to three histidines as clarified by an EXAFS study (16) indicated the catalytic role of the zinc in PAL.

In some enzymes possessing catalytic zinc such as alcohol dehydrogenase and carboxypeptidases A, B, and P (31), it has been reported that the zinc can be replaced with cobalt and cadmium for full activity. As indicated by Vallee and Galdes, the replacement of catalytic zinc with other metal ions can affect activity profoundly, whereas that of structural zinc atoms has only minor consequences (31). With PAL, it should be noted that the metal substitution largely altered the its kinetic properties; i.e., the Co and Cd substitution increased the $k_{cat}$ and the $K_m$ values about 3- and 5-fold, respectively, compared to those of the wild-type and the Zn$^{2+}$-reconstituted PAM (Table 3). In contrast, the $k_{cat}/K_m$ values of the Co- and Cd-substituted PAM are not so

different from that of the wild-type and Zn-reconstituted enzymes, thus indicating that the four enzyme species (wild-type, Zn-, Co-, and Cd-substituted enzyme) possess a similar catalytic ability regardless of the bound metal species. These observations together with the fact that various hydrated metals themselves catalyzed the decomposition of TNPYV(OH)G to TNPYV-NH$_2$ as a general base support the enzyme-bound zinc playing a catalytic role, rather than a structural role, in the PAL reaction. Also, it is likely that the restoration of the PAL activity by Co$^{2+}$ or Cd$^{2+}$ is a consequence of their binding to the catalytic site of the enzyme in a proper geometry.

Recently, De et al. suggested the presence of an iron−zinc bimetallic center and its possible involvement in the catalysis of PAL based on their observation that mutation of Tyr654 resulted in the complete loss of the enzyme activity and in marked depletion of iron and zinc. According to them, Tyr654 is involved in the formation of a phenolate−Fe(III) charge transfer complex, showing a characteristic broad absorption band around 560 nm (21). We have also observed a similar visible spectrum with our PAM preparations (data not shown). However, the involvement of iron in the catalysis appears less likely. First, PAL contains only substoichiometric amounts of iron, less than 0.2 mol/mol of enzyme (21). In contrast, the zinc content is constantly near stoichiometric. Second, the PAL activity is not influenced by the iron content that varies between the PAM preparations, and there is no correlation between the PAL activities and the intensity of the 560 nm band (K. Takahashi, S. Harada, and M. Noguchi, unpublished observation). Finally, if the iron constitutes a bimetallic center and acts catalytically, the metal should locate in close proximity to zinc within a distance of 4−5 Å. However, an EXAFS study did not show any trace of iron even in the outer shell of zinc (16). Therefore, we consider the role of iron to be questionable at present.

To summarize, in the present study we focused on the role of enzyme-bound metal in the PAL reaction. We presented, for the first time, evidence that various divalent metals catalyze the nonenzymatic decomposition of TNPYV(OH)G to TNPYV-NH$_2$ by acting as a catalytic base. We also showed the absolute requirement of enzyme-bound zinc in the PAL reaction by means of a metal-removal and -substitution study and suggested that the water molecule coordinated to the active site zinc may serve as a general base in the catalysis of PAL. However, a structural analysis of PAM is awaited with great interest for the further clarification of the PAL reaction.

## SUPPORTING INFORMATION AVAILABLE

The apparatus for the removal of enzyme-bound metals (Figure S1), calculation of the second-order rate constant ($k_2$) for the decomposition of TNPYV(OH)G to TNPYV-NH$_2$ by the basic form of the hydrated metal (Figure S2 and Table S1), and measurement of the second-order rate constant for the hydroxide ion-catalyzed decomposition of TNPYV(OH)G to TNPYV-NH$_2$ (Figures S3 and S4 and Table S2). This material is available free of charge via the Internet at http://pubs.acs.org.

## REFERENCES

1. Prigge, S. T., Mains, R. E., Eipper, B. A., and Amzel, L. M. (2000) New insights into copper monooxygenases and peptide amidation; structure, mechanism and function. *Cell. Mol. Life Sci. 57*, 1236–1259.
2. Eipper, B. A., Mains, R. E., and Glembotski, C. C. (1983) Identification in pituitary tissue of a peptide α-amidation activity that acts on glycine-extended peptides and requires molecular oxygen, copper, and ascorbic acid. *Proc. Natl. Acad. Sci. U.S.A. 80*, 5144–5148.
3. Zabriskie, T. M., Cheng, H., and Vederas, J. C. (1991) Incorporation of aerobic oxygen into the hydroxyglycyl intermediate during formation of *C*-terminal peptide amides by peptidylglycine α-amidating monooxygenase. *J. Chem. Soc., Chem. Commun.,* 571–572.
4. Noguchi, M., Seino, H., Kochi, H., Okamoto, H., Tanaka, T., and Hirama, M. (1992) The source of the oxygen atom in the α-hydroxyglycine intermediate of the peptidylglycine α-amidating reaction. *Biochem. J. 283*, 883–888.
5. Merkler, D. J., Kulathila, R., Consalvo, A. P., Young, S. D., and Ash, D. E. (1992) $^{18}$O isotopic $^{13}$C NMR shift as proof that bifunctional peptidylglycine α-amidating enzyme is a monooxygenase. *Biochemistry 31*, 7282–7288.
6. Katopodis, A. G., Ping, D., and May, S. W. (1990) A novel enzyme from bovine neurointermediate pituitary catalyzes dealkylation of α-hydroxyglycine derivatives, thereby functioning sequentially with peptidylglycine α-amidating monooxygenase in peptide amidation. *Biochemistry 29*, 6115–6120.
7. Takahashi, K., Okamoto, H., Seino, H., and Noguchi, M. (1990) Peptidylglycine α-amidating reaction: evidence for a two-step mechanism involving a stable intermediate at neutral pH. *Biochem. Biophys. Res. Commun. 169*, 524–530.
8. Perkins, S. N., Husten, E. J., and Eipper, B. A. (1990) The 108-kDa peptidylglycine α-amidating monooxygenase precursor contains two separable enzymatic activities involved in peptide amidation. *Biochem. Biophys. Res. Commun. 171*, 926–932.
9. Kato, I., Yonekura, H., Tajima, M., Yanagi, M., Yamamoto, H., and Okamoto, H. (1990) Two enzymes concerned in peptide hormone α-amidation are synthesized from a single mRNA. *Biochem. Biophys. Res. Commun. 172*, 197–203.
10. Eipper, B. A., Stoffers, D. A., and Mains, R. E. (1992) The biosynthesis of neuropeptides: peptide α-amidation. *Annu. Rev. Neurosci. 15*, 57–85.
11. Czyzyk, T. A., Ning, Y., Hsu, M., Peng, B., Mains, R. E., Eipper, B. A., and Pintar, J. E. (2005) Deletion of peptide amidation enzymatic activity leads to edema and embryonic lethality in the mouse. *Dev. Biol. 287*, 301–313.
12. Klinman, J. P. (1996) Mechanisms whereby mononuclear copper proteins functionalize organic substrates. *Chem. Rev. 96*, 2541–2561.
13. Tenn, W. J., French, N. L., and Nagorski, R. W. (2000) Kinetic dependence of the aqueous reaction of *N*-(hydroxymethyl)benzamide derivatives upon addition of electron-withdrawing groups. *Org. Lett. 3*, 75–78.
14. Bundgaad, H., and Kahns, A. H. (1991) Chemical stability and plasma-catalyzed dealkylation of peptidyl-α-hydroxyglycine derivatives, intermediates in peptide α- amidation. *Peptides 12*, 745–748.
15. Mennenga, A. G., Johnson, A. L., and Nagorski, R. W. (2005) General-buffer catalysis of the reaction of *N*-(hydroxymethyl)benzamide: a new pathway for the aqueous reaction of carbinolamides. *Tetrahedron Lett. 46*, 3079–3083.
16. Bell, J., Ash, D. E., Snyder, L. M., Kulathila, R., Blackburn, N. J., and Merkler, D. J. (1997) Structural and functional investigations on the role of zinc in bifunctional rat peptidylglycine α-amidating enzyme. *Biochemistry 36*, 16239–16246.
17. Kolhekar, A. S., Bell, J., Shiozaki, E. N., Jin, L., Keutmann, H. T., Hand, T. A., Mains, R. E., and Eipper, B. A. (2002) Essential features of the catalytic core of peptidyl-α-hydroxyglycine α-amidating lyase. *Biochemistry 41*, 12384–12394.
18. Eipper, B. A., Perkins, S. N., Husten, E. J., Johnson, R. C., Keutmann, H. T., and Mains, R. E. (1991) Peptidyl-α-hydroxyglycine α-amidating lyase: purification, characterization, and expression. *J. Biol. Chem. 266*, 7827–7833.
19. Satani, M., Takahashi, K., Sakamoto, H., Harada, S., Kaida, Y., and Noguchi, M. (2003) Expression and characterization of human bifunctional peptidylglycine α-amidating monooxygenase. *Protein Expression Purif. 28*, 293–302.

20. Kulathila, R., Consalvo, A. P., Fitzpatrick, P. F., Freeman, J. C., Snyder, L. M., Villafranca, J. J., and Merkler, D. J. (1994) Bifunctional peptidylglycine α-amidating enzyme requires two copper atoms for maximum activity. *Arch. Biochem. Biophys. 311*, 191–195.

21. De, M., Bell, J., Blackburn, N. J., Mains, R. E., and Eipper, B. A. (2006) Role for an essential tyrosine in peptide amidation. *J. Biol. Chem. 281*, 20873–20882.

22. Takahashi, K., Onami, T., and Noguchi, M. (1998) Kinetic isotope effects of peptidylglycine α-hydroxylating mono-oxygenase reaction. *Biochem. J. 336*, 131–137.

23. Takahashi, K., Satani, M., Harada, S., and Noguchi, M. (2003) Expression and characterization of frog peptidylglycine α-hydroxylating monooxygenase. *Protein Expression Purif. 27*, 35–41.

24. Mills, S. A., and Klinman, J. P. (2000) Evidence against reduction of $Cu^{2+}$ to $Cu^+$ during dioxygen activation in a copper amine oxidase from yeast. *J. Am. Chem. Soc. 122*, 9897–9904.

25. Agostinelli, E., De Matteis, G., Sinibaldi, A., Mondovi, B., and Morpurgo, L. (1997) Reactions of the oxidized organic cofactor in copper-depleted bovine serum amine oxidase. *Biochem. J. 324*, 497–501.

26. Suzuki, S., Sakurai, T., Nakahara, A., Manabe, T., and Okuyama, T. (1983) Effect of metal substitution on the chromophore of bovine serum amine oxidase. *Biochemistry 22*, 1630–1635.

27. Mounier, C. E., Shi, J., Sirimanne, S. R., Chen, B., Moore, A. B., Gill-Woznichak, M. M., Ping, D., and May, S. W. (1997) Pyruvate-extended amino acid derivatives as highly potent inhibitors of carboxyl-terminal peptide amidation. *J. Biol. Chem. 272*, 5016–5023.

28. Perrin, D. D. (1982) *Ionization constants of inorganic acids and bases in aqueous solution*, 2nd ed., Pergamon Press, New York.

29. Burgess, J. (1978) *Metal ions in solution*, Halsted Press, New York.

30. Vallee, B. L., and Auld, D. S. (1992) Active zinc binding sites of zinc metalloenzymes. *MATRIX Suppl. 1*, 5–19.

31. Vallee, B. L., and Galdes, A. (1984) The metallobiochemistry of zinc enzyme. *Adv. Enzymol. Relat. Areas Mol. Biol. 56*, 283–430.

32. Jackman, J. E., Raetz, C. R. H., and Fierke, C. A. (1999) UDP-3-*O*-(*R*-3-hydroxymyristoyl)-*N*-acetylglucosamine deacetylase of *Escherichia coli* is a zinc metalloenzyme. *Biochemistry 38*, 1902–1911.

33. Hernick, M., and Fierke, C. A. (2005) Zinc hydrolases: the mechanisms of zinc-dependent deacetylases. *Arch. Biochem. Biophys. 433*, 71–84.

34. Vallee, B. L., and Auld, D. S. (1990) Zinc coordination, function, and structure of zinc enzymes and other proteins. *Biochemistry 29*, 5647–5659.

35. Vallee, B. L., and Auld, D. S. (1993) Cocatalytic zinc motifs in enzyme catalysis. *Proc. Natl. Acad. Sci. U.S.A. 90*, 2715–2718.

36. Eriksson, A. E., Jones, T. A., and Liljas, A. (1988) The refined structure of human carbonic anhydrase II at 2.0 Å resolution. *Proteins 4*, 274–282.

37. Gomez-Ortiz, M., Gomis-Rüth, F. X., Huber, R., and Avilés, F. X. (1997) Inhibition of carboxypeptidase A by excess zinc: analysis of the structural determinants by X-ray crystallography. *FEBS Lett. 400*, 336–340.

38. Larsen, K. S., and Auld, D. S. (1991) Characterization of an inhibitory metal binding site in carboxypeptidase A. *Biochemistry 30*, 2613–2618.

39. Liaw, S. H., Chen, S. J., Ko, T. P., Hsu, C. S., Chen, C. J., Wang, A. H. J., and Tsai, Y. C. (2003) Crystal structure of D-aminoacylase from *Alcaligenes faecalis* DA1, a novel subset of amidohydrolases and insights into the enzyme mechanism. *J. Biol. Chem. 278*, 4957–4962.

40. Whittington, D. A., Rusche, K. M., Shin, H., Fierke, C. A., and Christianson, D. W. (2003) Crystal structure of LpxC, a zinc-dependent deacetylase essential for endotoxin biosynthesis. *Proc. Natl. Acad. Sci. U.S.A. 100*, 8146–8150.